

# Diffusion of Disperse Dye in Atactic Polystyrene

TORU MASUKO, MASAMI SATO,\* and MIKIO KARASAWA, *Faculty of Technology, Yamagata University, Yonezawa-shi, Yamagata-ken, 992 Japan*

## Synopsis

Sublimative desorption experiments were carried out on atactic polystyrene containing *p*-nitroaniline, *p*-aminoazobenzene, or C.I. Disperse Yellow 7 at 114°–170°C (above the  $T_g$  of the polymer). The diffusion coefficient of each dye in the polymer increased monotonically with rise in the desorption temperature. The mode of this change was exactly expressed by a WLF relation having the universal parameters given for amorphous polymers. The value of  $B_d$ , defined as the ratio of diffusional penetrant volume to that of a segment of the chain molecule, varied from 0.37 to 0.70 for the different dyes used. It is also shown that the  $B_d$  value is related to the logarithmic rotational volume of the dye molecule estimated from a molecular model.

## INTRODUCTION

It is generally considered<sup>1</sup> that a dye molecule diffuses in the amorphous region of a fiber through holes produced as the result of segmental motions, and the complexity of the dye diffusion mechanism in a dyeing process is caused by some factors that influence the segmental mobilities in the fiber structure. For instance, even in a dyeing system with a dye molecule that has comparatively weak affinity for a fiber, the existence of a crystalline region and orientated chains in the amorphous region depresses the amorphous chain mobilities to various extents, whereas water used as a dyeing medium penetrates into the fiber and consequently increases the mobility of the amorphous region.

Although many authors have extensively studied<sup>2</sup> the relations between dye diffusion and structural parameters, such as crystallinity, birefringence, x-ray orientation, and dynamic mechanical properties, these intricate factors make the elucidation of the dye diffusion mechanism more or less ambiguous.

Accordingly, it is necessary to study at first the dry system composed of a dye with weak affinity and an unoriented amorphous polymer in order to clarify the relation between dye diffusivity and segmental mobility, and then to extend the study to a more complex crystalline, wet polymer.

In the present study, the temperature dependence of the diffusion coefficient of some disperse dyes of various molecular sizes in dry atactic polystyrene is investigated in the temperature region above the glass transition temperature by means of a sublimative desorption method from the above-mentioned point of view. The diffusional behavior of the dye molecules is discussed in terms of the free-volume theory.

## EXPERIMENTAL

Polystyrene (PS) used in the present study was Styron 683, supplied by the Asahi Kasei Co., with molecular weight and density of  $2.4 \times 10^5$  and 1.06 g/cc,

\* Present address: The Yamagata Daiichi-Senko, Yamagata-shi, Yamagata-ken, 990 Japan.

respectively. The glass temperature ( $T_g$ ) of this polymer determined by a dilatometric method was 100°C. Model disperse dyes, *p*-nitroaniline (PNA) and *p*-aminoazobenzene (PAAB), were purified by recrystallization from water repeatedly and C.I. Disperse Yellow 7 (Y-7) was similarly recrystallized from methanol. The melting points of these dyes are shown in Table I.

Each dye was mixed with polystyrene pellets for 10 min on a hot roll heated at 180°C, which is higher than the melting point of every dye, and subsequently the mixture was molded into a film 0.1 mm thick ( $\pm 5\%$ ) by a hot press held at the same temperature. The film was then quenched in ice water. The weight ratios of dye to polystyrene ranged from 0.8/100 to 1.5/100. The dye concentration in the film was determined by a spectrophotometric method where the absorbance of a monochlorobenzene solution dissolving the colored film was measured at maximum wavelength ( $\lambda_{\max}$ ). The dye concentration at any part of the film was observed to be equal within experimental error, so that the dye was homogeneously dispersed in the polymer;  $\lambda_{\max}$  values of the dye solutions are also shown in Table I.

The glass temperatures of the colored films were measured on a differential scanning calorimeter (Shimazu DSC-30) using a baseline method<sup>3</sup> at a heating rate of 1°C/min and were found to be within  $100 \pm 2^\circ\text{C}$ . The temperatures almost agree with the result of pure polystyrene. Dye molecules, therefore, have negligible plasticizing effect on polystyrene in this concentration range.

The sublimative desorption apparatus employed in this study is similar to the equipment described by Ito et al.<sup>4</sup> Figure 1 shows schematically this apparatus in which two sublimation tubes are available simultaneously. A trap in the apparatus was cooled by liquid nitrogen so that one could keep the interior of the apparatus at a vacuum higher than  $10^{-3}$  torr during the sublimative desorption experiments. A strip  $1.5 \times 3.0$  cm<sup>2</sup> was cut out of the colored film and placed in a sublimation tube (Fig. 1, (7)) in such a manner that the strip was held flat with a holder made of stainless wire. Strips of 15–20 pieces were used to obtain one desorption curve.

The amount of dye desorbed during time  $t$  ( $M_t$ ) was estimated from ( $M_\infty - M_t'$ ), where  $M_\infty$  is the value of  $M_t$  for  $t = \infty$ , which was confirmed experimentally to be nearly equal to the dye concentration initially held in the film, and  $M_t'$  is the amount of the dye remaining in the film after desorption time  $t$ . The diffusion coefficient of the dye in the polymer film was calculated by<sup>4,8</sup>

$$D = \frac{\pi}{16} I^2$$

where

$$I = \frac{d(M_t/M_\infty)}{d(t^{1/2}/L)} \quad 0 < M_t/M_\infty < 0.6$$

TABLE I  
Some Characteristics of the Three Disperse Dyes

Dye	Solvent for purification	Tm., °C	$\lambda_{\max}$ in monochlorobenzene, m $\mu$
<i>p</i> -Nitroaniline (PNA)	H <sub>2</sub> O	145	350
<i>p</i> -Aminoazobenzene (PAAB)	H <sub>2</sub> O	126	377
C.I. Disperse Yellow 7 (Y-7)	CH <sub>3</sub> OH	167	390

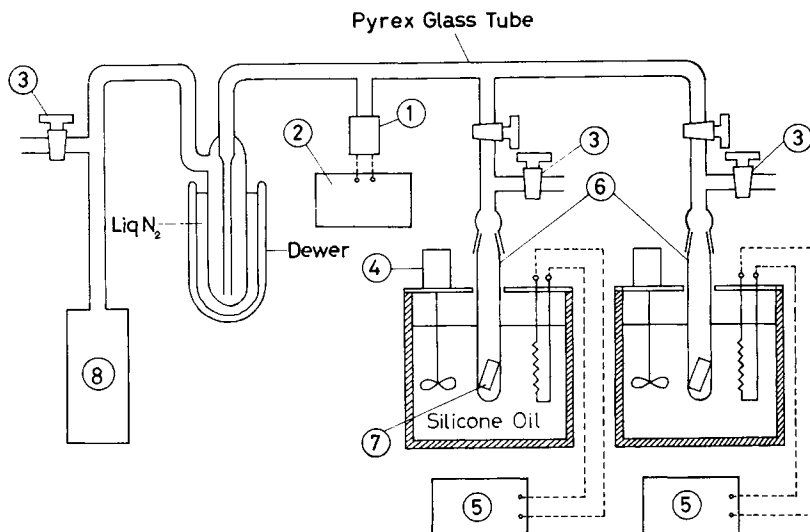


Fig. 1. Schematic representation of the desorption apparatus: (1) Pirani sensor; (2) vacuum indicator; (3) leak valve; (4) stirrer; (5) heater controller; (6) sublimation tube; (7) sample; (8) rotary pump.

$I$  is the initial slope of the reduced desorption curve and  $L$  is the film thickness, which was measured by an electrical micrometer after the desorption experiment. In order to obtain thermal equilibrium within the sample, all films were preheated in the sublimation tube for 3 min at the desorption temperature before a high vacuum was applied.

## RESULTS AND DISCUSSION

### Concentration Dependence of Diffusion Coefficient

Figure 2 shows the desorption of PAAB at 140°C where the concentration is changed from 5.1 to 12 mg dye/g polymer; all the points fall on a single reduced desorption curve within experimental error, giving a diffusion coefficient of  $2.13 \times 10^{-7} \text{ cm}^2/\text{min}$ . The result indicates the concentration dependence of PAAB diffusion to be negligible for such a small dye concentration.

Okajima et al. have already described that, in the investigations of the sublimative desorption of C.I. only. Disperse Red I and other disperse dyes in polyester<sup>4</sup> or polypropylene,<sup>5</sup> the concentration dependence of dye diffusion is extremely small in the dye concentration range below 45 mg dye/g polymer, and their results agree with those observed in the present PS-PAAB system. Hence, the concentration dependence of the dye diffusion coefficient was neglected throughout the present study.

### Temperature Dependence of Diffusion Coefficient

Reduced desorption curves of PNA, PAAB, and Y-7 at various sublimation temperatures are shown in Figures 3, 4, and 5, respectively. In comparison to the theoretical reduced desorption curves which are calculated by eq. (1)<sup>13</sup> (McBain's formula),

$$\frac{M_t}{M_\infty} = 1 - \frac{8}{\pi^2} \sum_{n=0}^{\infty} \frac{1}{(2n+1)^2} \exp\left(-\frac{(2n+1)^2 \pi^2 D t}{L^2}\right) \quad (1)$$

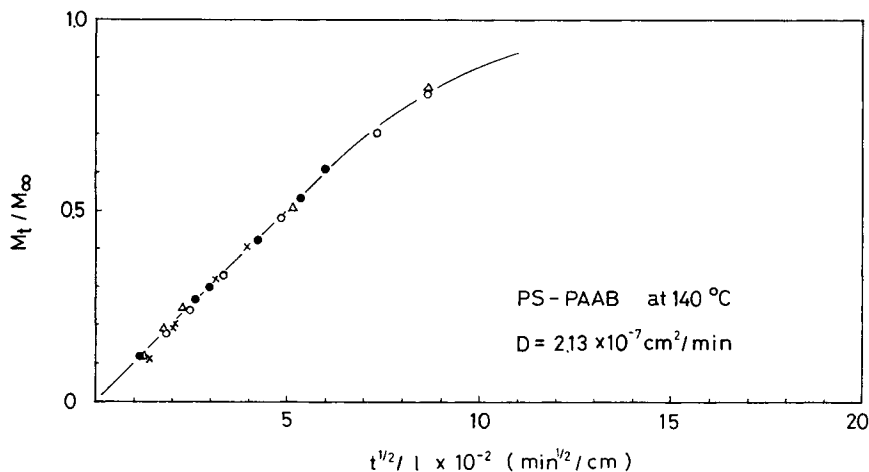


Fig. 2. Reduced desorption curve for *p*-aminoazobenzene at 140°C showing small concentration dependence of the diffusion coefficient: (●) 12.0 mg dye/g polymer; (Δ) 8.3; (○) 7.3; (×) 5.1.

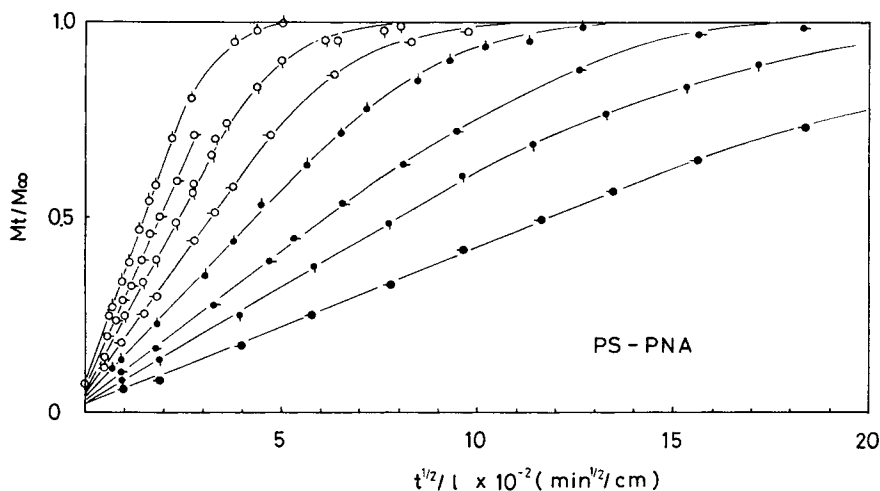


Fig. 3. Reduced desorption curves for *p*-nitroaniline at various temperatures: (◊) 150°C; (◌) 145°C; (◐) 140°C; (◑) 135°C; (●) 130°C; (◐) 125°C; (◑) 120°C; (●) 115°C.

all the experimental points of the PAAB in Figure 4 at 160°, 155°, 150°, 145°, and 141°C are in fairly good agreement with expression (1); it is evident, therefore, that the whole diffusion process is Fickian.

The logarithmic diffusion coefficients of these three disperse dyes as a function of the desorption temperature are shown in Figure 6, where  $\log D$  decrease monotonically with decrease in temperature. This feature is similar in these three dyes, and the curves are shifted toward each other along the temperature axis and superimposed into a single master curve which is displayed in Figure 7, with the PAAB curve as reference. The superposition is fairly good, and it is suggested that the segmental motion process in the polystyrene plays a principal role in transporting these dyes. The  $\Delta T$  quantity, the temperature shift for the superimposing operation, is in the order of 10°C.

The Arrhenius plot of  $\log D$  in Figure 6, as illustrated in Figure 8, reveals the monotonic decrease in  $\log D$  with increase in inverse absolute temperature

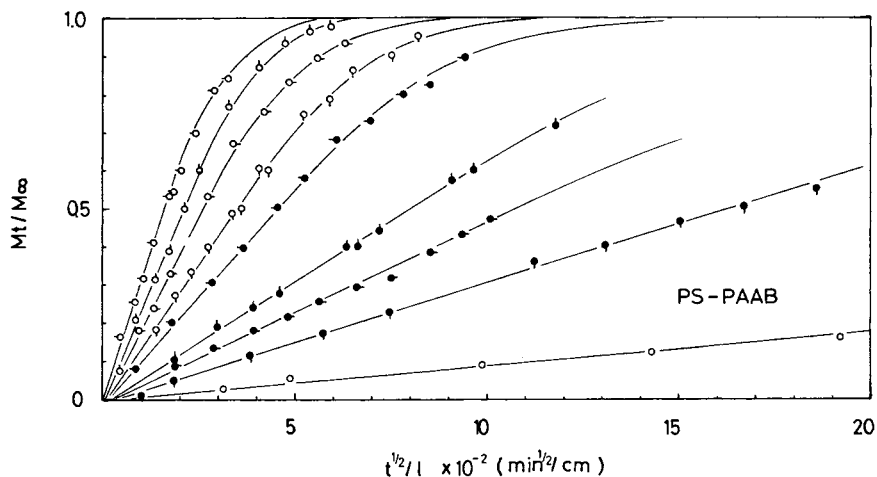


Fig. 4. Reduced desorption curves for *p*-aminoazobenzene at various temperatures: (○) 160°C; (◊) 155°C; (◐) 150°C; (◑) 145°C; (●) 141°C; (◐) 134°C; (◑) 130°C; (◐) 125°C; (○) 114°C.

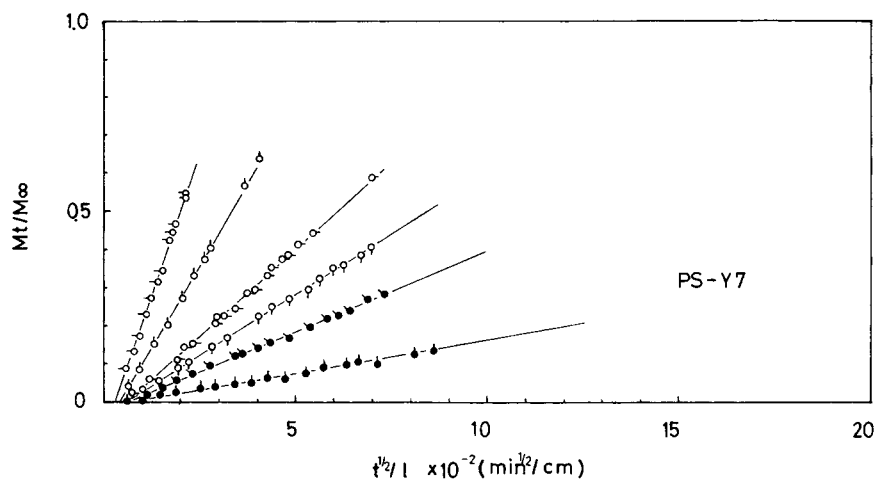


Fig. 5. Reduced desorption curves for C. I. Disperse Yellow 7 at various temperatures: (○) 170°C; (◊) 160°C; (◐) 150°C; (◑) 145°C; (●) 140°C; (◐) 130°C.

without any clear break points in this temperature range. The results are unlike those observed by Duda and Vrentas<sup>6</sup>; they found the  $T_{1,1}$  transition<sup>7</sup> of polystyrene at 150°C from the study of *n*-pentane diffusion. The reason for this discrepancy between the results of Duda and Vrentas and those of the present study is not clear.

One cannot obtain any definite activation energies of diffusion for the penetrants from the Arrhenius plots in Figure 8, and hence, in this case, it may be better to interpret the temperature dependence of the present dye diffusion coefficient by a free-volume approach rather than by an energy viewpoint.

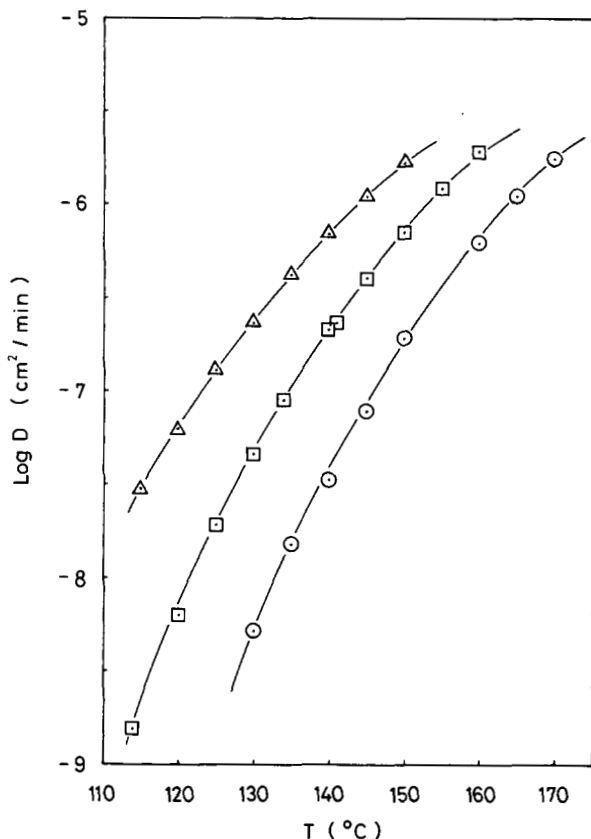


Fig. 6. Changes in diffusion coefficients for three disperse dyes as function of temperature: ( $\Delta$ ) PNA; ( $\square$ ) PAAB; ( $\circ$ ) Y-7.

### WLF-Type Equation in Diffusion

The diffusion coefficient of a penetrant in an amorphous polymer has been expressed by Fujita<sup>8</sup> in terms of the fractional free volume at temperature  $T$  as follows:

$$D_0 = RTA_d \exp(-B_d/f) \quad (2)$$

where  $D_0$  is the diffusion coefficient of the penetrant extrapolated to zero penetrant concentration,  $A_d$  and  $B_d$  are constants (especially the latter has been approximated as 0.6–0.8 from the experimental results of solvent diffusion in amorphous polymers), and  $R$  is the gas constant. If eq. (2) holds good at the glass transition temperature, where the fractional free volume is expressed as  $f_g$ , one obtains

$$\ln(D_0/D_{0g}) + \ln(T_g/T) = -B_d[(1/f) - (1/f_g)] \quad (3)$$

$f$  is generally considered to be a linear increase function of  $T$ , as in

$$f = f_g + \alpha_f(T - T_g) \quad (4)$$

where  $\alpha_f$  is the thermal expansion coefficient of free volume. In the case of  $D_0 \simeq D$ , a small concentration dependence of the diffusion coefficient on the penetrant, substitution of eq. (4) into eq. (3) yields the following expression:

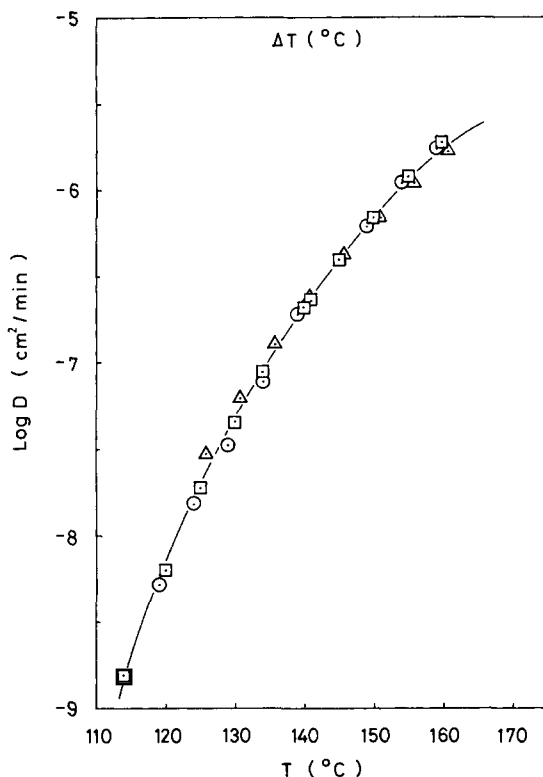


Fig. 7. Superposition of PNA and Y-7 curves on PAAB curve in relation to the temperature axis: ( $\Delta$ ) PNA, shifted +11°C; ( $\square$ ) PAAB; ( $\circ$ ) Y-7, shifted -11°C.

$$\begin{aligned}
 \log d_T^{\xi} &\equiv \log(D/D_g) + \log(T_g/T) \\
 &= (-B_d/2.3)[(1/f) - (1/f_g)] \\
 &= \frac{(B_d/2.3f_g)(T - T_g)}{(f_g/\alpha_f) + (T - T_g)} \\
 &= \frac{C_1^{gd}(T - T_g)}{C_2^{gd} + (T - T_g)} \quad (5)
 \end{aligned}$$

Equation (5) is of the WLF type,<sup>9</sup> where  $B_d/2.3f_g$  and  $f_g/\alpha_f$  are substituted by  $C_1^{gd}$  and  $C_2^{gd}$ , respectively, and  $D \cdot T_g/D_g \cdot T \equiv d_T^{\xi}$  denotes the temperature shift factor of diffusion with the  $T_g$  as reference temperature.

On the other hand, the value of the polymer viscosity  $\eta$  at  $T$  relative to the viscosity  $\eta_g$  at the  $T_g$ , which is generally defined as the temperature shift factor of viscosity, is expressed in terms of free volume as follows:

$$a_T^{\xi} \equiv \eta/\eta_g = \exp[(1/f) - (1/f_g)] \quad (6)$$

and then eq. (6) can be combined with eq. (5), yielding

$$\log d_T^{\xi} = -B_d \log a_T^{\xi}. \quad (7)$$

Equation (7) gives the  $B_d$  value if one can determine  $d_T^{\xi}$  and  $a_T^{\xi}$  independently, and  $\log a_T^{\xi}$  is calculated by using the universal values for viscosity at  $T_g$  in amorphous polymers, which are  $C_1^{\xi} = 1/2.3f_g = 17.44$  and  $C_2^{\xi} = f_g/\alpha_f = 51.6$ .<sup>9</sup> In case of a completely amorphous polymer,  $C_2^{gd}$  is expected to agree with  $C_2^{\xi}$  from

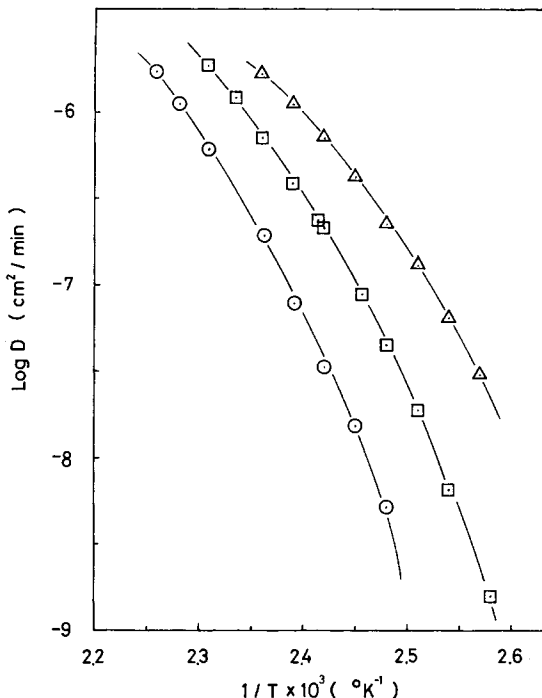


Fig. 8. Arrhenius plots of the diffusion coefficients for three disperse dyes. The data are taken from Figure 6.

the derivation of eq. (7). If one selects  $T_s = T_g + 50^\circ\text{C}$  as reference temperature instead of the  $T_g$ , eq. (5) is transformed into

$$\begin{aligned} \log d_T^s &\equiv \log (D/D_s) + \log (T_s/T) \\ &= \frac{C_1^{sd}(T - T_s)}{C_2^{sd} + (T - T_s)} \end{aligned} \quad (8)$$

where

$$\begin{aligned} C_1^{sd} &= C_1^{gd}C_2^{gd}/(C_2^{gd} + T_s - T_g) \\ C_2^{sd} &= C_2^{gd} + T_s - T_g \end{aligned} \quad (9)$$

On replotting the data in Figure 6, each plot of  $(T - T_s)/\log d_T^s$  versus  $(T - T_s)$  shows a good straight line, as displayed in Figure 9, where  $T_s$  is  $150^\circ\text{C}$ ; and one may obtain  $C_1^{sd}$  and  $C_2^{sd}$  from the slopes and intercepts (at  $T - T_s = 0$ ) of these lines. The values of  $C_1^{gd}$  and  $C_2^{gd}$  for these three dyes converted from the  $C_1^{sd}$  and  $C_2^{sd}$  data by using eq. (9) are collectively summarized in Table II. The value of  $C_1^{gd}$  increases with increase in the molecular size of the penetrant, while the  $C_2^{gd}$  value is nearly constant and equal to the universal value of 51.6. Upon reflection, it becomes apparent that the  $B_d$  values, calculated from eq. (7) and also shown in Table II, increase similarly with increase in molecular size. When  $f_g$  is assumed to be 0.025, the  $\alpha_f$  values, calculated from eq. (7), remain nearly constant for these dyes, in conformity with the universal value of  $4.8 \times 10^{-4} \text{ deg}^{-1}$  for viscosity.



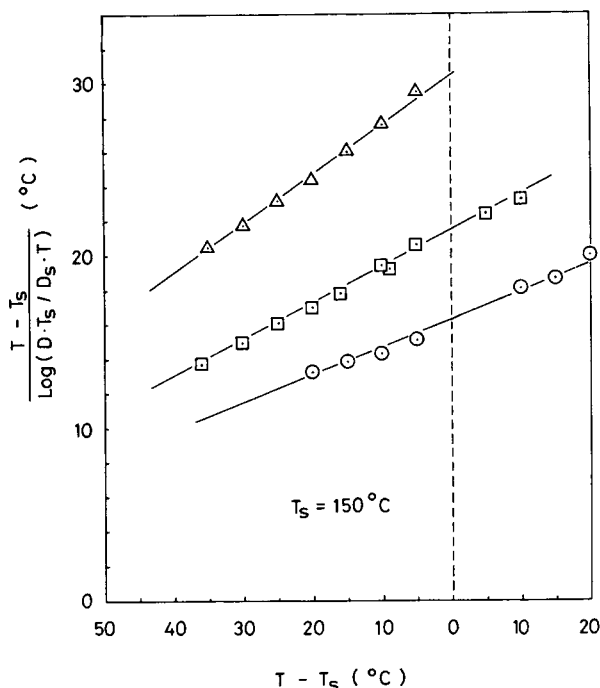


Fig. 9. Plots for determination of  $C_1^{gd}$  and  $C_2^{gd}$ : ( $\Delta$ ) PNA; ( $\square$ ) PAAB; ( $\circ$ ) Y-7.

TABLE II  
WLF Constants Obtained from Diffusion Data<sup>a</sup>

	$C_1^{gd}$	$C_2^{gd}$ , deg	$C_1^{gd} C_2^{gd}$ , deg	$\alpha_f \times 10^4$ , deg <sup>-1</sup>	$B_d$
Penetrant					
PNA	6.52	52.3	341	4.78	0.37
PAAB	9.27	51.6	478	4.84	0.53
Y-7	12.27	51.9	637	4.82	0.70
Segment	17.44	51.6	900	4.85	1.0

<sup>a</sup> The numerical values for the segment are the universal viscosity values.

### Relation Between $B_d$ and Molecular Volume

It is considered, therefore, that dye diffusion is strictly controlled by the free volume produced as the result of the thermal motion of polymer segments. The difference in the dye diffusion coefficients among these three dyes at the same temperature is essentially a function of the  $B_d$  value.

The  $B_d$  value is defined as the diffusional volume of a penetrant to that of a segment<sup>8</sup> (Cohen-Turnbull<sup>10</sup> and Bueche<sup>11</sup> ascribed rather different physical meaning to  $B_d$ , but in the present case we follow Fujita's idea). According to this definition, the  $B_d$  value equals unity when the diffusional volume of the penetrant agrees with that of the segment.

One can estimate the molecular volume of the dyes from the two-dimensional molecular size scaled by an H.G.S. molecular structure model (Maruzen Co.), as illustrated in Figure 10. Three values of rotational molecular axes selected

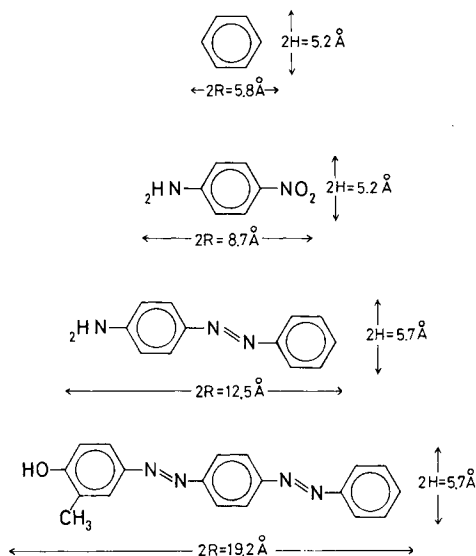


Fig. 10. Molecular dimensions of benzene and three disperse dyes. Numerical values are obtained from the H.G.S. molecular structure model (Maruzen Co.).

as shown in Table III. Logarithmic molecular volumes are expected to have some relation to the  $B_d$  value from Bueche's theory.<sup>11</sup>

Hence,  $B_d$  was plotted against the three kinds of logarithmic rotational volume for each dye molecule as shown in Figure 11. It is demonstrated that the relation is considerably linear for each model. The straight lines in Figure 11 are drawn without any difficulty in such a way that they cross in the vicinity of a molecular volume of  $130 \text{ \AA}^3$ . This volume corresponds incidentally to the volume of benzene averaged over the three shapes. The disperse dyes used in the present study have benzene-containing structures, and that is probably the reason why the  $B_d$ -versus- $\log V_d$  plots have a focus point around the volume of benzene ( $V_d$  is the rotational, logarithmic molecular volume of the dye).

When these straight lines are extrapolated to  $B_d = 1.0$ , the molecular volumes at the intercepts should give the approximate values of the segment size. The volumes of 1100, 8600, and  $30,000 \text{ \AA}^3$  are obtained from the plots of A (cylinder I), B (cylinder II), and C (sphere), respectively. In the last case, the segment

TABLE III  
Three Kinds of Rotational Molecular Volumes for Various Penetrants Calculated from the Numerical Values of Figure 10

Penetrant	Cylinder I (A) volume $2\pi H^2R, \text{ \AA}^3$	Cylinder II (B) volume $2\pi HR^2, \text{ \AA}^3$	Sphere (C) volume $4/3\pi R^3, \text{ \AA}^3$	
Benzene	$H = 2.6 \text{ \AA}$ $R = 2.9 \text{ \AA}$	123	137	102
PNA	$H = 2.6 \text{ \AA}$ $R = 4.4 \text{ \AA}$	184	309	345
PAAB	$H = 2.9 \text{ \AA}$ $R = 6.3 \text{ \AA}$	319	699	1023
C.I. Disperse Yellow 7	$H = 2.9 \text{ \AA}$ $R = 9.6 \text{ \AA}$	490	1650	3706

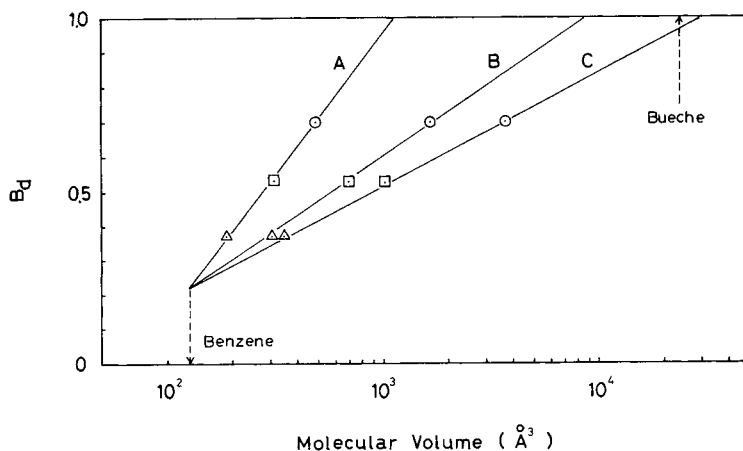


Fig. 11. Plots of  $B_d$  vs logarithmic molecular volume. A, B and C correspond to the different choices of rotational axes: (A) cylinder I; (B) cylinder II; (C) sphere.

volume is of the same order as Bueche's estimate from viscosity data<sup>12</sup> (his estimated value was  $24,000 \text{ \AA}^3$ ). If one considers the substantial agreement of the estimated segment volume between diffusion and viscosity to have some physical significance, it can be assumed that, in the dye diffusion process, the penetrant sweeps a spherical volume in the amorphous polymer, and the diffusion coefficient of the penetrant is determined by the ratio  $B_d$  relating this penetrant-sweeping volume to the effective free volume for diffusion produced by the segmental motion of the polymer.

### Conclusions

The diffusion coefficients of the three disperse dyes (PNA, PAAB, and Y-7) in amorphous polystyrene are observed to change with the variation in free volume resulting from the segmental motion of the polymer. The temperature dependence of the dye diffusivity is quantitatively described by a WLF-type relation with reasonable constants. The  $B_d$  values in this study vary from 0.37 to 0.70 as the penetrant volume changes. These values are found to be related to the rotational molecular volumes of the penetrant. Further studies along this line will be required to establish whether the relationship holds good in other polymer-penetrant systems.

The authors wish to thank Professor S. Okajima of the North Shore College, Atsugi-shi, Kanagawa-ken, for his advice and earnest discussion on interpreting the  $B_d$  value. They also acknowledge the Asahi Kasei Company for the supply of polystyrene.

### References

1. R. H. Peters, in *Diffusion in Polymers*, J. Crank and G. S. Park, Eds., Academic Press, London, 1968, Chap. 9, p. 315.
2. R. H. Peters, in *Textile Chemistry*, Vol. III, Elsevier, London, 1975, Chap. 21, p. 681.
3. M. S. Ali and R. P. Sheldon, *J. Appl. Polym. Sci.*, **14**, 2619 (1970).
4. I. Ito, S. Okajima, and F. Shibata, *J. Appl. Polym. Sci.*, **14**, 551 (1970).
5. S. Okajima, N. Sato, and M. Tasaka, *J. Appl. Polym. Sci.*, **14**, 1563 (1970).
6. J. L. Duda and J. S. Vrentas, *J. Polym. Sci. A-2*, **6**, 675 (1968).
7. R. F. Boyer, *J. Polym. Sci.*, **C14**, 267 (1966).

8. H. Fujita, *Fortschr. Hochpolym.-Forsch.*, **3**, S1 (1961).
9. M. L. Williams, R. F. Landel, and J. D. Ferry, *J. Am. Chem. Soc.*, **77**, 3701 (1955).
10. M. H. Cohen and D. Turnbull, *J. Chem. Phys.*, **31**, 1164 (1959).
11. F. Bueche, in *Physical Properties of Polymers*, Interscience, New York, 1962, Chap. 4, p. 85.
12. F. Bueche, *J. Chem. Phys.*, **21**, 1850 (1953).
13. J. Crank, in *The Mathematics of Diffusion*, 2nd ed., Clarendon Press, Oxford, 1975, Chap. 4, p. 48.

Received December 8, 1976

Revised February 11, 1977